Pergamon

Solid State Communications, Vol. 105, No. 5, pp. 297–300, 1998

0038–1098/98 $19.00+.00

PII: S0038–1098(97)10125-9

MEASUREMENT OF THE ELASTIC MODULUS OF A MULTI-WALL BORON NITRIDE NANOTUBE

Nasreen G. Chopra and A. Zettl

Department of Physics, University of California at Berkeley and Materials Science Division, Lawrence Berkeley National Laboratory, Berkeley, CA 94720, U.S.A.

(*Received* 16 *September* 1997; *accepted* 7 *October* 1997 *by S.G. Louie*)

We have experimentally determined the elastic properties of an individual multi-wall boron nitride (BN) nanotube. From the thermal vibration amplitude of a cantilevered BN nanotube observed in a transmission electron microscope, we find the axial Young's modulus to be 1.22 ± 0.24 TPa, a value consistent with theoretical estimates. The observed Young's modulus exceeds that of all other known insulating fibers. Our elasticity results confirm that BN nanotubes are highly crystalline with very few defects. © 1998 Elsevier Science Ltd

The discovery [1–4] of various types of nanotubes has provided fertile ground for both experimental and complementary theoretical studies. For pure carbon nanotubes, theoretical calculations predict that electrical properties range from semiconducting to metallic depending upon the radius and chirality of the tube [5, 6]. Similar results are obtained for BC_2N and BC_3 nanotubules (for BC_3 the electrical properties of a tube bundle are in addition sensitive to tube–tube interactions) [7, 8]. In contrast, all BN nanotubes are predicted [9] to be semiconductors with a uniform large gap regardless of the radius, chirality, or the number of walls of the tube. This makes BN nanotubes particularly useful for applications where a high-strength fiber of uniform electronic structure is desired. For carbon and other nanotubes, such application is difficult as there is presently no successful process for isolating tubes with similar electrical properties.

High resolution transmission electron microscopy (TEM) images of carbon, BN and other nanotubes show clear lattice fringes suggesting a high degree of crystallinity. Calculations [10, 11] of the elastic properties of ideal carbon nanotubes predict an exceptionally high axial Young's modulus (of order 1–6 TPa) due to the strong in-plane bonding of the nanostructures. Indeed, recent experiments on both multi-walled [12, 13] and single-walled carbon nanotubes [13] have confirmed these theoretical predictions. Similar predictions apply to BN nanotubes where preliminary calculations [14] indicate for pure BN nanotubes a Young's modulus 0.95 times the ideal carbon nanotube elastic modulus. The exceptional mechanical strength (and associated high sound velocity, high thermal conductivity, etc.) of nanotubes, coupled to desirable electrical properties, presents a unique physical system.

We here report on measurements to determine the elastic properties of BN nanotubes. Since measurements on random collections of nanotubes often do not reflect single tube properties, experiments on individual nanotubes, specifically characterized by TEM, are most desirable. We thus explored several methods for measuring the elastic properties of individual nanotubes *in situ* inside a high resolution transmission electron microscope, including measuring the deflection due to external forces applied to a nanotube (deflections due to gravitational and "electron wind" forces are negligible); determining the resonant frequency of a particular tube by driving it with a forced oscillator; and measurement of the thermal vibration amplitude of a cantilevered nanotube. The thermal excitation method is the most straightforward to implement and is the technique reported on here. This method has been recently used by Treacy *et al.* [12] to measure the Young's modulus of multi-wall carbon nanotubes.

BN nanotubes were synthesized by arcing a BN filled tungsten rod against a water-cooled copper electrode in an arc-discharge chamber with parameters previously described elsewhere [3]. This method produced pure BN multi-walled nanotubes which were characterized

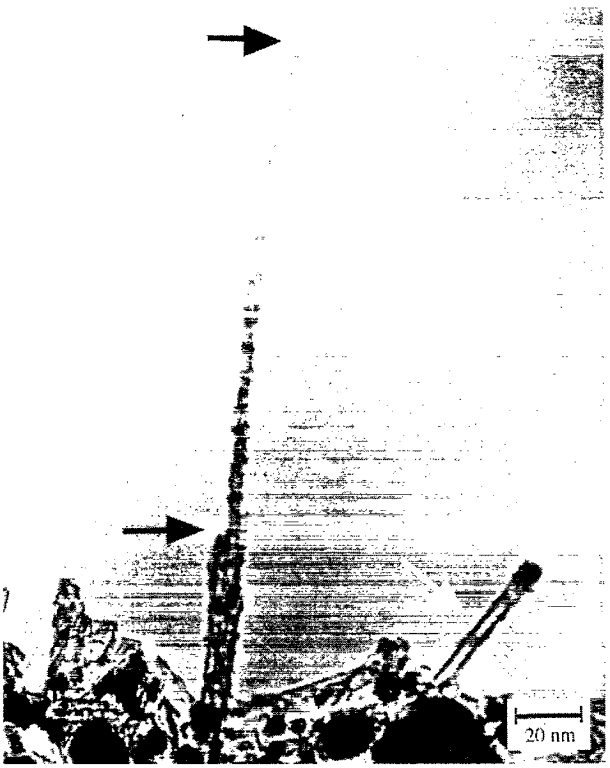

Fig. 1. Transmission electron micrograph of BN nanotube at 300 K. The black arrows identify the supported base and tip of a long cantilevered nanotube; the tip region is markedly blurred due to thermally-induced vibrations of the nanotube. The white arrow identifies another BN nanotube whose thermally induced vibration amplitude is too small to be resolved.

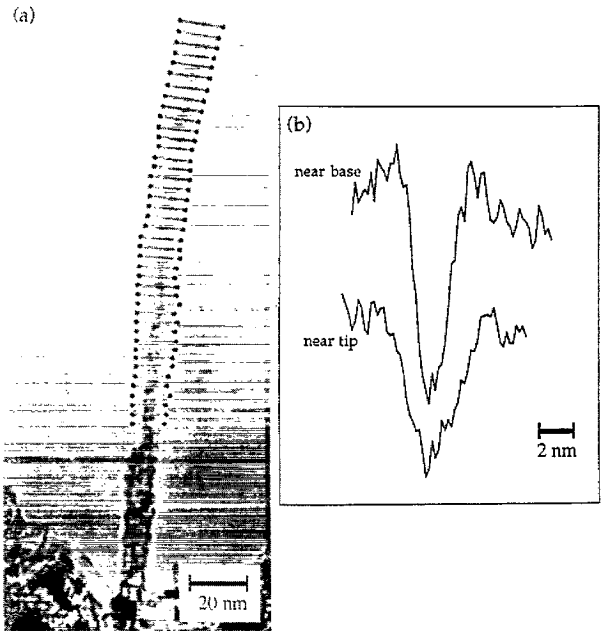

Fig. 2. Line scan analysis of vibrating BN nanotube image. (a) The placement of the horizontal bars represents the position at which line scans were taken on the image of a single BN nanotube (same one as Fig. 1). (b) Plots of the contrast variation across the width of the tube at regions near the base and near the tip.

by high resolution TEM and electron energy loss spectroscopy, confirming the crystalline nature and composition of the tubules. BN nanotubes synthesized by this technique often contain metal particles at the ends. The BN nanotubes were placed on copper/amorphous carbon support grids and imaged at 300 K in a high resolution TEM using 200 keV electrons.

Figure 1 is a TEM micrograph of a BN nanotube specimen. Two individual BN nanotubes are clearly visible, both cantilevered over a hole in the support grid. A short BN tube in the lower right region of the image (identified by the white arrow) has a clearly visible metal particle at its tip; the entirety of the tube is in clear focus indicating a small thermal vibration amplitude. The central region of Fig. 1 shows a single long cantilevered BN nanotube. The base (lower black arrow) of this nanotube is in clear focus, while closer to the tip region (upper black arrow) the image becomes successively more blurred. We performed a focus plane and rotation study to verify that the blurring of the tip region is thermal in origin and not due to sample tilt. We also insured that the image remained unchanged with decreasing electron flux (and thus decreasing electron beam heating), confirming a nanotube sample temperature close to 300 K.

To quantify the amplitude of the vibration modes of the nanotube in the image plane, a series of intensity line scans perpendicular to the nanotube axis was performed on the micrograph of Fig. 1. Figure 2(a) indicates the positions of the scans (short horizontal bars). Figure 2(b) shows two representative intensity scans, one near the supported base and one near the nanotube tip. The region of intensity below the baseline in these traces represents the time averaged intensity contrast of the vibrating nanotube, from which the vibration amplitude can be determined. The width of the nanotube at the base, where the vibration amplitude falls to zero, is 3.5 nm.

Figure 3 shows the rms transverse nanotube vibration amplitude as a function of distance from the nanotube base, determined from a deconvolution of the intensity line scans from the base line scan. As expected, the vibration amplitude increases with increasing distance from the clamped base of the nanotube. Although not measured, identical nanotube vibrations are expected in the direction perpendicular to the imaging plane. Longitudinal (axial) and torsional vibration modes could not be resolved (as expected). Transverse intensity scans were also performed on the smaller BN tube of

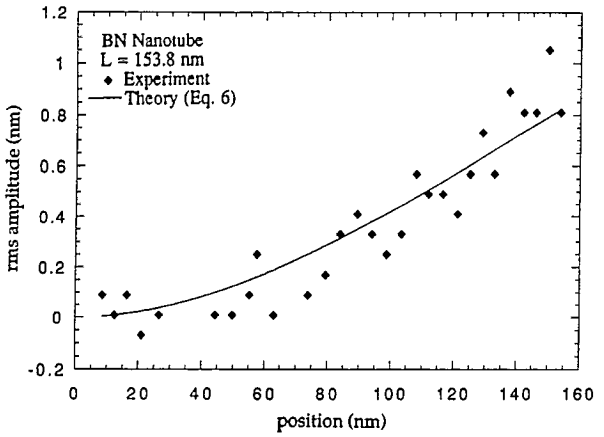

Fig. 3. r.m.s. amplitude of oscillation as a function of position from the base of the BN determined from the line scans. The solid line shows the best fit using the normal modes of a thermally-excited cantilever, equation (6).

Fig. 1; thermally excited vibrations could not be resolved. Using elastic constants excited for BN nanotubes (see below), the maximum vibration amplitude for this short nanotube is calculated to be on the order of 0.05 nm, beyond our detection limit.

The magnitude and functional form of the vibration amplitude data of Fig. 3 allow an explicit determination of the elastic properties of BN nanotubes. Our analysis is motivated by that of Treacy *et al.* performed for multi-walled carbon nanotubes [12]. However, in the analysis of Treacy *et al.*, the vibration amplitude is experimentally measured only at one point (the tube tip), while in our analysis we exploit the full measurement of the vibration amplitude functional form. We approximate the nanotube as a cantilevered Bernoulli–Euler beam of length L with a uniform circular cross section of outer diameter a, inner diameter b and mass per unit length μ, rigidly clamped at one end and freely vibrating at the other. The continuum approximation averages over the discreet B and N atoms in the longitudinal and radical directions. However, because of the relatively long nanotube length and finite shear modulus between concentric nanotube shells, the error in making this continuum approximation is small. The displacement $u(x, t)$ of the vibrating nanotube is described as a superposition of normal modes

$$u(x,t) = \sum_{n=1}^{\infty} u_n(x,t) = \sum_{n=1}^{\infty} z_0 \alpha_n \phi_n(x) \sin \omega_n t, \tag{1}$$

where z_0 is the maximum amplitude and α_n is the relative amplitude of the normal mode $\phi_n(x)$ at frequency ω_n. The complete set of normalized normal modes of a cantilevered beam is given by [15]

$$\phi_n(x) = \frac{1}{2}\left[\cosh \beta_n x - \cos \beta_n x - \frac{\cosh \beta_n L + \cos \beta_n L}{\sinh \beta_n L + \sin \beta_n L}(\sinh \beta_n x - \sin \beta_n x)\right], \tag{2}$$

with $\beta_n = 1.8751, 4.6941, 7.8548, 10.996$ for $n = 1, 2, 3, 4$ and approximately $(2n-1)\pi/2$ for $n > 4$. The Young's modulus Y is embedded in the associated frequency expression

$$\omega_n = (\beta_n L)^2 \sqrt{\frac{YI}{\mu L^4}} = (\beta_n L)^2 \sqrt{\frac{Y\pi(a^4 - b^4)}{64\mu L^4}}, \tag{3}$$

where the second moment of area $I = \pi(a^4 - b^4)/64$ for a hollow circular cross section [15].

In order to extract a value for Y from the experimental data, we consider the energy of the system. From the equipartition theorem, the average kinetic energy in each available mode is $k_B T/2$ where k_B is Boltmann's constant and T is the temperature. The average kinetic energy of a given mode is

$$\langle E_n^{\text{kinetic}} \rangle = \int_0^L \tfrac{1}{2}\mu[\dot{u_n}(x,t)]^2 \, dx = \tfrac{1}{2}\mu\omega_n^2 z_0^2 \alpha_n^2 \int_0^L [\phi_n(x)]^2 \, dx \langle(\sin \omega_n t)^2\rangle. \tag{4}$$

Equating equation (4) to $\frac{1}{2}k_B T$

$$\alpha_n = \sqrt{\frac{8k_B T}{\mu\omega_n^2 z_0^2 L}} = \frac{1}{(\beta_n L)^2}\sqrt{\frac{512L^3 k_B T}{Y\pi(a^4 - b^4)z_0^2}}, \tag{5}$$

hence

$$u(x,t) = \sqrt{\frac{512L^3 k_B T}{Y\pi(a^4 - b^4)}}\left[\sum_{n=1}^{n_{max}} \frac{1}{(\beta_n L)^2}\phi_n(x) \sin \omega_n t\right]. \tag{6}$$

The equipartition theorem fixes the relative mode amplitudes: $\alpha_1 : \alpha_2 : \alpha_3 : \alpha_4 \ldots = 1 : 0.16 : 0.057 : 0.03 \ldots$. The amplitudes of higher order modes fall off as $\sim 1/n^2$. Hence the vibration amplitude profile is dominated by the first few modes. The higher order modes become unimportant well before the quantum accessibility of the modes comes into question; the summation in equation (6) is ultimately limited at room temperature at $n_{max} \approx 85$ where $h\omega_{n_{max}} \approx k_B T$.

The solid line in Fig. 3 is a best fit of the rms vibration amplitude predicted by equation (6) to the experimental data for the BN nanotube. A reasonable fit is obtained, supporting the assumptions of the model, the superposition of normal modes and the applicability of the equipartion theorem. The model and the experimental

data reveal the dominance of the first mode in the response of a cantilevered beam driven by a stochastic process. From the fit in Fig. 3 (solid line), we find the maximum rms amplitude of oscillation to be 0.8 nm. This fit, together with the measured dimensions of the nanotube, $a = 3.5$ nm, $b = 2.2$ nm and $L = 153.8$ nm, yields an elastic modulus of $Y = 1.22$ TPa for the BN nanotube at $T = 300$ K. The largest uncertainty in the value of Y arises from uncertainties in geometrical dimensions. We estimate uncertainties in a and b of roughly 0.1 nm and in L of roughly 0.1 nm. This leads to an uncertainty in the absolute value of Y of order $\pm 20\%$. The vibration frequency of the fundamental mode of the long BN nanotube of Fig. 1 is calculated to be $\omega_1 \approx 2$ GHz.

As mentioned previously, BN nanotubes synthesized by the tungsten-arc technique often terminate with a dense metal particle. If we assume the long BN nanotube of Fig. 1 is terminated by a tungsten particle with a diameter on the order of the outer tube diameter and repeat the analysis, the fundamental frequency is decreased by 17%. However, the BN tube elastic modulus does not change. This is consistent with the simplest mass-spring system where the oscillation frequency depends on the mass and elastic constant of the spring, but the spring constant is independent of the mass as long as the spring is within the linear extension limit.

Our value of $Y = 1.22 \pm 0.24$ TPa for BN nanotubes is in the range of what has been observed for conducting multiwalled carbon nanotubes (0.4–4 TPa [12], 1.3 TPa [13]) and single-walled carbon nanotubes (4 TPa for a single single-walled tube and 0.35 TPa for a hypothetical close-packed array of such tubes, including the "space" between the tubes [13]) and to our knowledge it greatly exceeds the elastic modulus of any known insulating fiber. For comparison, Y for fibers of E-glass, Kevlar 49 and silicon carbide are 73.5 GPa [17], 112 GPa [18] and 200 GPa [19], respectively. The BN nanotube Young's modulus is 14 times greater than the measured in-plane modulus of bulk hexagonal BN material [20]. This difference is possibly due to the tube being a defect-free single crystalline entity while the bulk hexagonal material is a composite of defected layers. Our experiment shows the impressive change in elastic properties of a material due to nanometer scale sample geometry. Hexagonal BN is well-known for its high temperature resistance which is expected to carry over to BN nanotubes. Thus, BN nanotubes have exceptional thermal, electrical and mechanical properties.

Acknowledgements—We thank R.J. Luyken for assistance in sample synthesis and A.K. Chopra, K. Khazeni, Ari Mizel and M.S. Fuhrer for useful discussions and M.A. O'Keefe of the National Center for Electron Microscopy, Lawrence Berkeley National Laboratory, for helpful interactions. This work was supported by the U.S. Department of Energy under Contract No. DE-AC03-76SF00098 and by the Office of Naval Research, Order No. N00014-95-F-0099. NGC acknowledges support from a Department of Education Graduate Fellowship and AZ acknowledges support from the Miller Institute for Basic Research in Science.

REFERENCES

1. Ijima, S., *Nature*, **354,** 1991, 56.
2. Weng-Sieh, Z. *et al.*, *Phys. Rev.*, **B51,** 1995, 11229.
3. Chopra, N.G. *et al.*, *Science*, **269,** 1995, 966.
4. Loiseau, A., Willaime, F., Demoncy, N., Hug, G. and Pascard, H., *Phys. Rev. Lett.*, **76,** 1996, 4737.
5. Hamada, N., Sawada, S.-i. and Oshiyama, A., *Phys. Rev. Lett.*, **68,** 1992, 1579.
6. Saito, R., Fujita, M., Dresselhaus, G. and Dresselhaus, M.S., *Appl. Phys. Lett.*, **60,** 1992, 2204.
7. Miyamoto, Y., Rubio, A., Cohen, M.L. and Louie, S.G., *Phys. Rev.*, **B50,** 1994, 4976.
8. Miyamoto, Y., Rubio, A., Louie, S.G. and Cohen, M.L., *Phys. Rev.*, **B50,** 1994, 18360.
9. Blase, X., Rubio, A., Louie, S.G. and Cohen, M.L., *Europhys. Lett.*, **28,** 1994, 335.
10. Ross, P.E., *Scientific American*, **24,** 1991.
11. Overney, G., Zhong, W. and Tomanek, D., *Z. für Phys.*, **D27,** 1992, 93; Yakobson, B.I., Brabec, C.J. and Bernholc, J., *Phys. Rev. Lett.*, **76,** 1996, 2511.
12. Treacy, M.M., Ebbesen, T.W. and Gibson, J.M., *Nature*, **381,** 1996, 678.
13. Chopra, N., University of California, Berkeley PhD Thesis, 1996.
14. Angel Rubio (private communication).
15. Chopra, A.K., *Dynamics of Structure*, p. 592. Prentice Hall, New York, 1995.
16. Popov, E.P., *Engineering Mechanics of Solids*, p. A-4. Prentice Hall, New York, 1990.
17. Marotzke, C., *Compos. Sci. Technol.*, **50,** 1994, 393.
18. Barsoum, M.W., Kangutkar, P. and Wang, A.S.D., *Compos. Sci. Tech.*, **44,** 1992, 257.
19. DuPont, *Kevlar Aramid Fiber*, p. II-2. DuPont Advanced Fibers Systems, Wilmington, DE, U.S.A. 1992.
20. Data supplied by Carborundum Corporation, Latrobe, PA, U.S.A.